

# Parameter Estimation Bias From Overlapping Binary Black Hole Events In Second Generation Interferometers

Philip Relton<sup>1,\*</sup> and Vivien Raymond<sup>1</sup>

<sup>1</sup>*Gravity Exploration Institute, Cardiff University, Cardiff CF24 3AA, United Kingdom*

(Dated: March 1, 2025)

Since the initial detection of Gravitational Waves in 2015, 50 candidate events have been reported by the LIGO-Virgo-KAGRA collaboration. As the current generation of detectors move towards their design sensitivity the rate of these detections will increase. The next generation of detectors are likely to have high enough sensitivities that multiple merging binaries will be visible at the same time. In this paper we show that this is likely to happen before the end of the decade, with the move to the LIGO-Voyager detector. We investigate the situation of overlapping Binary-Black-Hole mergers in these detectors. We find that current parameter estimation techniques are capable of distinguishing the louder of two merging BBH events, without significant bias, when their merger times are not less than  $\sim 0.1$  seconds apart and when the ratio of the signal-to-noise ratios of the systems is uneven. This region of overlapping parameter space is dependent upon the sky locations of the signals and the relation of those locations to the light travel time between detectors. We also find that, if two signals are highly overlapping, then the recovered set of parameters often show strong evidence of precession. Finally we show that bias can occur even when the signal causing the bias is below the detection threshold.

## I. INTRODUCTION

In 2015 the Advanced LIGO (aLIGO) detectors [1] and the Advanced Virgo detector [2] began their first observing runs [3, 4]. Over a year of observations; a Binary Neutron Star, BNS, merger [5] and eleven Binary Black Hole, BBH, mergers were observed [6], at a rate of roughly one per five weeks. After another year of upgrades [7–9], the combined LIGO-Virgo-KAGRA (LVK) Collaboration observed 39 mergers within six months of observing time. This is a rate of roughly one merger per 1.5 weeks [10]. Candidates for further events have been reported, using LIGO-Virgo data from the first two observing runs, by groups external to the LVK Collaboration [11–14]. As Gravitational Wave, GW, detectors progress to their design sensitivity [1], and are replaced with more advanced detectors [15–19], the viewing range of the detectors will increase. This in turn will increase the rate of binary mergers.

As the rate of observed mergers increases, the probability of more than one, concurrent signal being observable by the network increases. Most current detection and analysis techniques assume that only one signal is visible at any period of time. Therefore, any overlapping signals would be assumed to be one single signal. As such, if overlapping signals start to make up a significant portion of detected signals, this difference could significantly bias wider reaching studies such as

population modelling and tests of General Relativity. Even a single overlapping event could negatively affect scientific results if the bias from the second signal causes significant deviation.

In this paper we investigate the probability of observing two compact binary mergers at close enough times that their waveform's interfere while observable in the detector. Previous studies [20, 21] have performed this calculation numerically and have focused on third generation detectors (3G), such as Einstein Telescope [17, 18] and Cosmic Explorer [19]. Here we calculate this analytically, including results for second generation detectors and proposed end of generation detectors such as LIGO-Voyager [15, 22].

We also investigate the effects overlapping signals can have on parameter estimation techniques currently in use within the LVK Collaboration. Previous studies into overlapping signals have investigated the bias caused when attempting to recover either of the two signals in the data [20, 21]. For our analysis, we treat overlapping signals as a single event and apply parameter estimation agnostically, making only the assumption that the system is a merging BBH. We attempt to constrain the regions in which such overlapping signals show significant bias. We also show what forms this bias can take when simple precessing waveforms and black hole spin parameters are included.

We show the calculation of the probability of overlapping observations section II. We then outline our method of signal overlap and recovery in section III. The results of this study are described in section IV, with updates on our probability calculation from our

---

\* Correspondence email address: reltonpj@cardiff.ac.uk

results in section V. Section VI provides a summary of our findings and proposals of avenues for further study.

## II. PROBABILITY

### A. Probability of Observing Overlapping Events

The number of Compact-Binary-Coalescence (CBC) events observed by a detector depends on the volume of space that the detector can observe, the merger rate of such systems and the length of observing period. By taking a power spectral density (PSD) of a detector, it is possible to characterise the noise of that detector and to use this to calculate the Signal-to-Noise-Ratio (SNR) of a particular compact binary coalescence.

As CBC mergers are assumed to be random and independent, they can be modelled by a Poisson distribution. The probability of an merging system being observed within a specific time period is then given by:

$$P(k \text{ events in time } T_{\text{obs}}) = \frac{(R T_{\text{obs}})^k \exp^{-RT_{\text{obs}}}}{k!} \quad (1)$$

where  $R$  is the rate of mergers,  $T_{\text{obs}}$  is the period of observation,  $k$  is the number of mergers in that period. To observe two mergers that overlap in time, there must be two events that occur within the period of a single signal,  $T_{\text{signal}}$ . With this period we can use Poisson statistics to calculate the inter-arrival time for two events. If the first event occurs at time  $t_0$  and the second event occurs at time  $t_1 = t_0 + \Delta T$ , then we can find the probability that  $\Delta T$  is less than the observable period of a signal  $T_{\text{signal}}$ :

$$P(\Delta T < T_{\text{signal}}) = 1 - \exp^{RT_{\text{signal}}} \quad (2)$$

We can also calculate the probability of two events overlapping for the period of a single event. We can use Equation 1 to find the probability that two or more events occur within the period of a single merger:

$$P(k \geq 2) = 1 - P(k = 0) - P(k = 1) \quad (3)$$

This can then be used to calculate the number of events that will contain an overlap in the life of a detector. By multiplying the probability of overlapping events being present in a period by the number of those periods in the observing run we can estimate the number of possible overlapping events in the whole observing run.

Current estimates on the merger rate of compact binaries are confined to redshifts of  $z \lesssim 1$  due to the nature of observed events. It is possible that this rate will increase with increasing redshift [23]. An increase in the rate of detections would lead to an increase in the rate of overlapping signals. However, for the purposes of our study we have assumed a constant merger rate, regardless of redshift. In addition, apart from Einstein Telescope, all detectors studied here all have viewing ranges of less than  $z \lesssim 1$ .

To estimate the distance at which a particular detector configuration can observe different merging systems we use the BNS range. The 'BNS-range' of a detector is, by convention, the distance at which the detector can observe a binary neutron star coalescence (BNS) with masses  $1.4M_{\odot} - 1.4M_{\odot}$  at an SNR of 8. The equivalent, conventional, 'BBH-range' for binary black hole mergers (BBH) is for two  $30M_{\odot}$  black holes at an SNR of 8. The mean BNS range for the first part of the third observing run, O3, were 108 Mpc and 135 Mpc for LIGO: Hanford and LIGO: Livingston respectively [10]. Estimates of the BBH range, prior to the start of O3, indicate it should have been in the range 990 – 1200 Mpc [24].

### B. Probability of Overlapping BBH Mergers

The rates and populations paper from the second gravitational wave transient catalogue produced by the LVK collaboration estimated the rate of BBH mergers from the events it observed at:  $R_{\text{BBH}} = 23.9_{-8.6}^{+14.9} \text{ Gpc}^{-3} \text{ yr}^{-1}$  [23].

The increasing sample of observed BBH mergers allows for the rate of merger to be calculated as a function of the systems component masses [23]. We used publicly available data [25] to draw a sample of merging systems with known component masses, this distribution is described in detail in fig 19 of [23]. From this sample of events we can calculate the average period over which a BBH merger will be visible to aLIGO detectors. We assumed a low frequency cut off of 20 Hz for this calculation.

The predicted BBH distance for the next observing run, O4, of aLIGO is 1600 Mpc [24]. With the current estimate of the BBH merger rate, this predicts the observation of  $98_{-35}^{+61}$  events in a year of observations. Combining this rate of observations with our estimate of the average observable BBH period and Equation 2, we can estimate the probability of observing overlapping events in this observing run, to approximately  $1.9 \times 10^{-5}_{-6.7 \times 10^{-6}}^{+1.2 \times 10^{-5}}$ . As expected, it is quite unlikely that such an event will occur during the next observing

run.

However, when aLIGO is replaced by the proposed LIGO-Voyager detector [15, 16] the sensitivity, and therefore viewing range, will increase to about 4100 Mpc. This range was calculated by creating a model PSD of the LIGO-Voyager detector. The PSD was created using the python package `pygwinc` to predict the noise budgets for such a detector and from that the expected sensitivity [26]. We then used the `inspiral-range` package to predict the BBH range of the detector from this PSD [27, 28]. LIGO-Voyager is expected to have a low frequency cut off of 10 Hz. This increases the observable period for BBH signals, further increasing the probability of overlap.

With this detector configuration, the number of mergers in a years observing run is  $1700^{+1000}_{-600}$ . The probability of observing overlapping signals in LIGO-Voyager is approximately 0.2%. This could occur in as many as  $2^{+2}_{-1}$  of observable BBH detections in LIGO-Voyager. This could be a significant number of events, particularly if the bias from the overlap causes drastic changes to the recovered signal parameters. As LIGO-Voyager is likely the first time we will see overlapping events these overlapping BBH cases are what we have focused on in this study.

By the mid 2030s, 3G detectors, such as Einstein Telescope (ET), will start their observation runs. These detectors will have almost an order of magnitude better sensitivity and much lower frequency cut offs, allowing for longer observable periods. Observing overlapping signals here is certain and should account for all BBH mergers. Values for these calculations are given in Table II D.

### C. Probability of Overlapping BNS Mergers

The BNS merger rate is not well constrained due to the unknown distribution of neutron star masses. To date the LVK collaboration has only observed two BNS mergers [5, 29]. To calculate the average period of their merger we defined a probability distribution function for the mass of the primary Neutron star and drew a random sample. The distribution was a truncated normal distribution between  $1 M_{\odot}$  and  $3 M_{\odot}$  with a mean of  $1.4 M_{\odot}$  and variance 0.5. From this sample we drew masses for primary object; and then the secondary object with the constraint that  $mass 2 \leq mass 1$ . These two distributions can be seen in Figure 1

With a random sample of component masses we calculated the average merger time for BNS signals. Again with a low frequency cut off of 20 Hz. BNS signals have much lower mass than BBH and as such

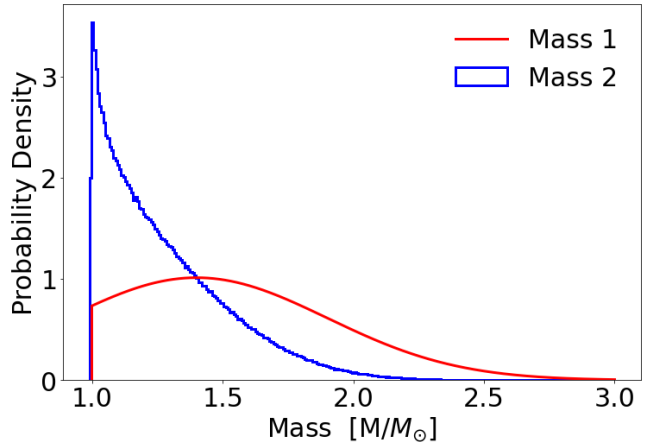


FIG. 1. Distribution of primary mass, red, secondary mass, blue, for BNS mergers

merge at much higher frequencies. The signals are often present in the detector for several minutes.

Following the same method as before we can use this average visible merger time to calculate the probability of two or more overlapping signals occurring in O4. The rate of BNS mergers is  $R_{BNS} = 320^{+490}_{-240} \text{ Gpc}^{-3} \text{ yr}^{-1}$  [23], the expected BNS distance is 190 Mpc [24]. Therefore the predicted number of observed BNS mergers in O4 is  $2^{+4}_{-1}$  mergers per year. Over the full year of O4 the probability of detecting two signals from BNS events that overlap is  $1.2 \times 10^{-5}^{+1.8 \times 10^{-5}}_{-8.9 \times 10^{-6}}$ .

Due to the still relatively high low frequency cut off there is a very low chance of observing overlapping BNS signals in LIGO-Voyager. However, the increase in sensitivity in 3G detectors, combined with the much lower low frequency cut off, will lead to a large number of overlapping BNS systems. It is likely that most, if not all, BNS mergers will overlap. This is mostly due to the increased number of observable cycles. Values for these calculations are given in Table II D.

### D. Probability of BBH Mergers Overlapping with BNS Mergers

BBH mergers visible in ground based interferometers for much shorter periods. The visible period for a standard  $30 + 30 M_{\odot}$  BBH merger in aLIGO is approximately 0.894 seconds, for a standard  $1.4 - 1.4 M_{\odot}$  BNS merger this is 160.8 seconds. However, at the sensitivities of aLIGO & LIGO-Voyager, BBH signals are observed at a much higher rate. It is therefore most

likely that overlapping events will be observed with a BBH merger occurring within the visible period of a BNS inspiral.

We calculate this probability, using the method described in section II A, to be  $5.3 \times 10^{-4}^{+3.3 \times 10^{-4}}_{-1.9 \times 10^{-4}}$  for the next observing run of aLIGO. It is possible that such events would be observed before the end of the current aLIGO detectors. They are likely to account for around 3% of all BBH mergers in LIGO-Voyager, as many as  $46^{+72}_{-27}$  overlapping events in a year. Values for these calculations are given in Table II D.

However, our analysis shows that there should not be significant problems in distinguishing these signals in the case of an overlap. There are large differences between the frequency evolution's of these kinds of CBC mergers. These differences, particularly as most of these BBH signals will merge long before the BNS signal merges, should cause the two events to be distinguishable. The section of the signal containing the merging BBH can be rejected as has been done for glitches present in BNS signals [5]. Due to this, we do not present any analysis into these types of overlap here.

### E. Other Mergers

The Advanced LIGO and Advanced Virgo detectors are sensitive to several other gravitational wave sources. Neutron Star-Black Hole mergers have yet to be have been conclusively observed by LIGO [10, 30, 31]. This limits the accuracy of estimating these merger rates. To the same extent very high mass collisions, such as Intermediate Mass Black Hole mergers (IMBH), are rare enough to make their merger rates difficult to predict. These signals are also much shorter, further reducing the chances of signal overlaps. For these reasons we do not consider these events any further in this study.

As yet no GW event from an observed Supernovae has been announced by the LVK collaboration. It is of course possible that these events could overlap. However, we do not consider these due to lack of any observations.

Considering the large number of events we expect to see in Einstein Telescope, we examine the probability of observing more than two signals at the same time. This is possible by extending Equation 3 to the case of  $N$  overlapping events:

$$P(k > N) = 1 - \sum_{k=0}^{k=N} P(k) = 1 - \sum_{k=0}^{k=N} \frac{(RT_{obs})^k \exp^{-RT_{obs}}}{k!} \quad (4)$$

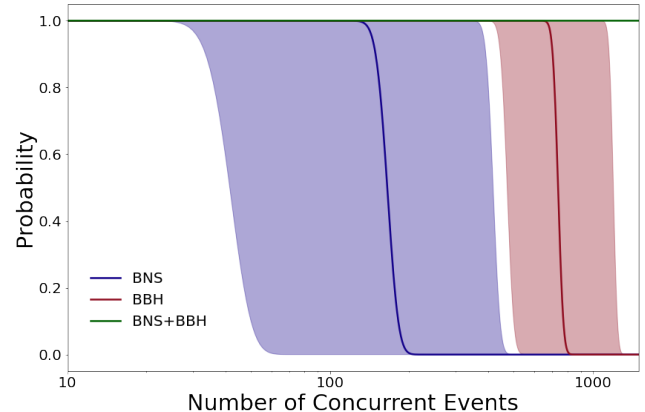


FIG. 2. Probability distribution for the likely number of BNS, blue, and BBH, red, mergers that overlap with each other. For BNS+BBH events, the probability of observing  $N$  or more of BBH events that overlap a visible BNS is 1 until much higher values than those presented here. This is shown by the green horizontal line at  $P(N > k) = 1$

We calculated the probability for every value of  $N$  up to 10,000 for three kinds of events; BBH, BNS and BNS+BBH, using the rate and viewing range estimates given in Tables II D, II D, II D respectively. We predict that at least  $110^{+220}_{-100}$  BNS mergers will overlap each BNS merger, for BBH mergers there are likely to be  $630^{+430}_{-240}$  overlapping each individual BBH. These results are shown in Figure 2.

Figure 2 indicates that each BNS signal is almost certain to overlap with more than 1500 BBH events. Our calculations find this is true beyond  $N = 10,000$ . A reasonable estimate of this value is to calculate the value directly from period of a BNS signal and estimates of the numbers of BBH mergers in a years ET observation. By multiplying the predicted number of BBH mergers in an observing period with the fraction of the observing period that contains the single BNS, this estimate can be found as approximately  $21000^{+13000}_{-7400}$  events.

It follows from these findings that it is unlikely Einstein Telescope will be able to observe any signal that doesn't overlap multiple other events. However, the probability of observing  $P(k > 2)$  in second generation detectors such as aLIGO or LIGO-Voyager is negligible. Therefore, it is reasonable to consider the two signal situation for these detectors.

Our results in section IV constrain the regions of parameter space in which two signals cause significant bias. In section V we re-estimate the number of overlapping signals based upon our bias-causing parameter

Detector	BBH Range (Mpc)	$f_{low}$ (Hz)	Period (s)	$P(Overlap_{BBH})$	$N_{events}$ (BBH)	$N_{Overlap}$ (BBH) <sup>†</sup>
aLIGO: O3[24]	1200	20	5.97	$7.8 \times 10^{-6+4.9 \times 10^{-6}}_{-2.8 \times 10^{-6}}$	$41^{+26}_{-15}$	$0^{+0}_{-0}$
aLIGO: O4[24]	1600	20	5.97	$1.9 \times 10^{-5+1.2 \times 10^{-5}}_{-6.7 \times 10^{-6}}$	$98^{+61}_{-35}$	$0^{+0}_{-0}$
aLIGO: Design[24]	2500	20	5.97	$7.1 \times 10^{-5+4.4 \times 10^{-5}}_{-2.5 \times 10^{-5}}$	$370^{+230}_{-130}$	$0^{+0}_{-0}$
LIGO-Voyager[22]	4100	10	38.46	$2.0 \times 10^{-3+1.3 \times 10^{-3}}_{-7.3 \times 10^{-4}}$	$1700^{+1000}_{-600}$	$2^{+2}_{-1}$
Einstein Telescope[17]	38000	1	17740.0	$1.00^{+0.00}_{-0.00}$	$1300000^{+820000}_{-470000}$	$1800^{+0}_{-0}$

TABLE I. The probabilities of detecting overlapping BBH signals, and estimates on the number of such detections, in different GW detector configurations, across a years observations. <sup>†</sup> This is the number of distinct events that contain an overlap. Therefore, two events that are concurrent in the detector will be counted as a single event. In the case of Einstein Telescope, the signals are so frequent, and visible for such long periods of time, that it is unlikely that any event will be solely visible in the detector. This leads to the number of overlapping events equaling the number of average length signals that fit in the observing run length.

Detector	BNS Range (Mpc)	$f_{low}$ (Hz)	Period (s)	$P(Overlap_{BNS})$	$N_{events}$ (BNS)	$N_{Overlap}$ (BNS) <sup>†</sup>
aLIGO: O3[24]	1200	20	170.6	$3.8 \times 10^{-6+5.8 \times 10^{-6}}_{-2.9 \times 10^{-6}}$	$1^{+1}_{-1}$	$0^{+0}_{-0}$
aLIGO: O4[24]	1600	20	170.6	$1.2 \times 10^{-5+1.8 \times 10^{-5}}_{-8.9 \times 10^{-6}}$	$2^{+4}_{-1}$	$0^{+0}_{-0}$
aLIGO: Design[24]	2500	20	170.6	$6.2 \times 10^{-5+9.5 \times 10^{-5}}_{-4.7 \times 10^{-5}}$	$11^{+18}_{-8}$	$0^{+0}_{-0}$
LIGO-Voyager[22]	4100	10	1079.0	$4.3 \times 10^{-3+6.6 \times 10^{-3}}_{-3.3 \times 10^{-3}}$	$130^{+200}_{-95}$	$0^{+2}_{-0}$
Einstein Telescope[17]	38000	1	496000.0	$1.00^{+0.00}_{-0.00}$	$10500^{+16000}_{-7900}$	$64^{+0}_{-0}$

TABLE II. The probabilities of detecting overlapping BNS signals, and estimates on the number of such detections, in different GW detector configurations, across a years observations. <sup>†</sup> This is the number of distinct events that contain an overlap. Therefore, two events that are concurrent in the detector will be counted as a single event. In the case of Einstein Telescope, the signals are so frequent, and visible for such long periods of time, that it is unlikely that any event will be solely visible in the detector. This leads to the number of overlapping events equaling the number of average length signals that fit in the observing run length.

space and apply this to LIGO-Voyager and Einstein Telescope.

## F. Beyond Third Generation Detectors

In the mid 2030s a space based Gravitational Wave interferometer is planned to be launched. The LASER Interferometer Space Antenna, LISA, detector [32] is planned to have a much lower sensitivity than aLIGO. However, the detector is designed to observe a different frequency range than ground based detectors. Sensitive between the  $10^{-5}$  Hz and  $10^{-1}$  Hz band, it should observe the mergers of much more massive objects than LIGO. These more massive signals, such as Super Massive Black Hole mergers, will be much slower than LIGO BBH mergers. The result is hundreds, if not thousands, of overlapping signals. We do not consider these in this work.

## G. Validation of Analytical Probability Calculation

Previous studies of the probability of observing overlapping signals have considered a similar analytic approach to this calculation [20]. Others have considered a more numerical approach [21]. For completeness, we here check our result numerically in a similar method to that described in section 2 of [21].

From the same distributions as described in Sections II B and II C we draw samples of component masses. For each event we calculate the observable period and assign a merger time drawn from a uniform distribution across a years observing period. We then count how many signals in that observing period overlap in time. This process is repeated  $10^6$  times to obtain a reasonable average for each run. The resulting number of overlaps and  $P(\text{overlap})$  is approximately identical to the analytical result. We can therefore conclude that the numbers from our analytical study are correct, given current rate estimates.

Detector	BNS+BBH Range (Mpc)	$f_{low}$ (Hz)	Period (s)	$P(Overlap_{BNS+BBH})$	$N_{events}$ (BNS+BBH)	$N_{Overlap}^{\dagger}$ (BNS+BBH)
aLIGO: O3[24]	1200	20	170.6	$2.2 \times 10^{-4+1.4 \times 10^{-4}}$ $-8.0 \times 10^{-5}$	$41^{+26}_{-15}$	$0^{+0}_{-0}$
aLIGO: O4[24]	1600	20	170.6	$5.3 \times 10^{-4+3.3 \times 10^{-4}}$ $-1.9 \times 10^{-4}$	$98^{+61}_{-35}$	$0^{+0}_{-0}$
aLIGO: Design[24]	2500	20	170.6	$2.0 \times 10^{-3+1.3 \times 10^{-3}}$ $-7.3 \times 10^{-4}$	$370^{+230}_{-130}$	$0^{+1}_{-0}$
LIGO-Voyager[22]	4100	10	1079.0	$5.5 \times 10^{-2+3.3 \times 10^{-2}}$ $-2.0 \times 10^{-2}$	$1700^{+1000}_{-600}$	$46^{+72}_{-27}$
Einstein Telescope[17]	38000	1	496100.0	$1.00^{+0.00}_{-0.00}$	$1300000^{+820000}_{-470000}$	$64^{+0}_{-0}$

TABLE III. The probabilities of detecting a BBH signal while a BNS signal is present in the detector, and estimates on the number of such detections, in different GW detector configurations, across a years observations. Here the BNS+BBH range is the observable BNS range for that configuration, but the rate is that of BBH events.  $^{\dagger}$  This is the number of distinct events that contain an overlap. Therefore, two events that are concurrent in the detector will be counted as a single event. In the case of Einstein Telescope, the signals are so frequent, and visible for such long periods of time, that it is unlikely that any event will be solely visible in the detector. This leads to the number of overlapping events equaling the number of average length signals that fit in the observing run length.

### III. METHOD

#### A. Parameter Estimation of Gravitational Waves

The primary signal analysis technique performed in GW analysis is parameter estimation (PE). Parameter estimation uses stochastic sampling to select a set of parameters that best describe the CBC merger. At each step of the parameter estimation the sampler creates a random sample of probable parameter values. The posterior probability,  $P(h(t)|d(t))$ , of such a signal being present in the data is then calculated via Bayes Theorem:

$$P(h(t)|d(t)) = \frac{P(h(t))P(d(t)|h(t))}{P(d(t))} \quad (5)$$

where  $P(h(t))$  is the prior probability that a signal,  $h(t)$  could exist.  $P(d(t))$  is the evidence, the probability distribution of the data,  $d(t)$ .  $P(d(t)|h(t))$  is the likelihood, the probability of observing the signal in the data.

Possible signals are created through waveform approximations. These waveforms estimate the signal strain in the detector from the set of parameters that the sampler has drawn. The appearance of the waveform depends on the set of parameters that describe the system and the waveform approximation selected. These parameters are divided into two groups, intrinsic and extrinsic.

The intrinsic parameters describe the internal dynamics of the merging binaries. These include the chirp mass,  $\mathcal{M}_c$ , mass ratio,  $q$ , and six parameters describing the spins of the compact objects. The extrinsic parameters describe the system relative to the detector.

These include the luminosity distance of the system  $d_L$ , the relative inclination of the orbital plane, sky location in right ascension and declination, the phase,  $\phi$ , of the wave at arrival, the polarisation of the wave and the time of arrival. This set of 15 parameters must be selected in order to produce possible waveforms for the signal.

For this analysis we used the precessing waveform IMRPhenomPv2 [33–36] to best describe the features of the BBH mergers. More recent waveforms, as described in [37–40], allow for more accurate physical descriptions of systems. To follow standard convention we use the IMRPhenomPv2 waveform to keep the majority of this physics without drastically increasing the computational cost.

In PE, spin is often represented in terms of more generic spin parameters. In this paper we will refer to  $\chi_p$ , the precessing spin parameter. This describes the in-plane spin of the two black holes. See [41] for a more detailed explanation of this parameter. Parameter estimation of BBH mergers with little to no precessing spin generally return a posterior matching the given prior, or a posterior close to zero with small positive deviations. If it is constrained away from zero it is an indication that the spins of the component black holes are likely to be precessing about the orbital angular momentum vector of the system.

Certain parameters can be removed from the sampling by marginalising over the likelihoods of those parameters [42]. This reduces the number of parameters in the integral for the likelihood without large uncertainties in the recovered likelihood. In this study we perform PE with marginalization over the parameters of time, distance and phase. The sampling was performed with marginalisations over time, phase and

distance. Phase marginalisation is not always possible with precessing waveforms, creating likelihoods that can differ from the true likelihood. However, PhenomPv2 contains both (2,2) multipoles in the co-precessing frame [33]. This allows for precession to be measured with marginalisation over phase.

### B. Studying Overlapping Signals

In the case of a detected signal, current data analysis techniques assume only the presence of a single signal in the noise. We perform our analysis on a similar basis, in which the data segments containing one or more signals are treated as single events. However, if two or more GWs are present in the detector at the same time their signals will interfere and produce a non-physical resultant waveform. The sampling software will then select sets of parameters that match this waveform rather than those of the component signals.

For the scope of this study we restrict overlaps to two signals. The observed waveform is therefore comprised of two component signals, Signal A and Signal B, where Signal A is the primary waveform that remains constant throughout the analysis. We perform parameter estimation on a variety of combinations of the two signals and observe the situations in which the sampler recovers signals that differ significantly from the true posterior of either signal. Throughout our analysis we keep Signal A to be a GW150914-like merger with chirp mass of approximately  $28.1 M_{\odot}$  and mass ratio 0.806.

There are four main differences that can describe two overlapping signals: Relative merger time, the time separation between Signal A and Signal B's mergers. We control this separation in our analysis by manually setting a displacement of Signal B's merger time upon signal creation. For the majority of our analysis, we keep this separation constant between detectors by giving the two signals the same sky location. This is of course an unlikely situation, but should have little affect on the outcome of the PE for those studies. For our primary analysis we allow the merger time of Signal B to vary according to  $\Delta t_{\text{merger}} : [-0.1, 0.1]\text{seconds}$ , relative to the merger time of Signal A.

The second relative parameter compares the SNRs of the two signals, how loud Signal B is in comparison to Signal A. In order to vary this; we keep Signal A at a constant SNR of 30 throughout the whole analysis. The SNR of 30 was set for the LIGO: Hanford detector. The SNR in LIGO: Livingston was 24.3. We then vary the luminosity distance of Signal B such that it would independently appear at several, usually lower, SNRs in the detector. For our primary analysis we al-

lowed  $\text{SNR}_B : [5, 30]$ , for the LIGO: Hanford detector, in order to vary from very low relative SNRs to almost equal.

The third relative parameter is the difference in the two signals true waveform's. The frequency evolution of each waveform is described uniquely by it's own set of parameters. To this extent we describe the frequency evolution of each signal by controlling its chirp mass,  $\mathcal{M}_c$ . The chirp mass dominates the first Post Newtonian expansion and as such has a large effect on the frequency evolution of the waveform. To observe how this changes overlaps we vary Signal B's chirp mass according to  $\mathcal{M}_c : [24.1, 32.1] M_{\odot}$  giving a wide range around that of Signal A. The mass ratio of Signal B was kept constant at 0.9.

The frequency evolution of the two signals is also dominated by their initial phases. For our analysis, we keep Signal A's phase constant and perform several sets of analysis for each configuration of Signal B at different random phases.

We have restricted all analysis to overlapping BBH events. This was done we expect these types of overlap to cause the most significant bias in parameter estimation. From preliminary studies we also found that overlapping BBH events could show precession-like effects. Even when the component signals contained little to no precession.

Other studies [20, 21] have looked at overlapping BNS events and BBH events that merge during a visible BNS signal. For the sake of reducing computational time we have left these studies for future analysis. However, we expect that BNS+BBH mergers are less likely to cause significant bias due to their vastly different frequency evolution's. Unless the SNR of the BBH signal is very high relative to the BNS, sampling will likely recover the BNS correctly when given priors for the BNS, due to the much larger number of cycles. The signal will remain clean for much of its observable period. If recovery of the BBH is desired then unless the relative SNR is very large then it is likely that no reliable PE can be performed in this situation.

For the recovery a constant set of priors was used throughout the study. These priors were kept as close as possible to those outlined in Appendix C of [6], in order to best match initial analysis that would be performed in the event of a detection trigger.

To fully encompass the parameters of both systems, some of these priors were widened slightly. The luminosity distance prior was set with an upper limit of 6000 Mpc in order to cover the large luminosity distance of the lowest mass Signal B at SNR 5.

It is possible that the interference of the waveforms could cause merger like effects earlier in the period of

the signal. Therefore, the merger time prior was also widened from 0.2 seconds to 1 second. This was done in order to encompass the full chirps of each signal. This would allow for any signals that might interfere in such a way to cause chirp like characteristics far from the true merger.

The runs were all performed with signals injected in the commonly used "zero-noise" approximation where the noise is assumed to be identically zero across all frequencies. The resultant obtained posteriors are then expected average posterior under a large number of noise realisations. In addition we performed runs with Gaussian noise added to the signal to ensure consistency in our zero-noise results. None of these runs differed qualitatively from the posteriors found in the zero noise case and all conclusions held.

## IV. RESULTS

### A. Single Detector Runs

Our primary analysis considered overlapping events as seen in a single detector. Events are rarely published if only found in a single detector, however, this can occur in the event of an interesting event. This is possible for an event which has been significantly biased by an overlapping signal.

For each run; two signals were generated as described in section III, Signal B was then injected into the same data frame as Signal A using the python package GWpy [43]. The created data frames were then given to the parameter estimation software, BILBY, [44] using the nested sampler *Dynesty* [45]. The data segments were treated as potential observed BBH events with no further assumptions. This was done in order to match the detection process as would occur in the event of such overlapping events. The PSD used for these runs is the aLIGO Design PSD, from the column "Design" of the Table given in [46].

We find that in the case of an uneven SNR ratio, ratio of the SNRs of the two signals, the sampler will recover parameters much closer to those of the louder signal. The sampler can almost always correctly recover Signal A in the situation where its SNR is more than three times the SNR of Signal B. The results are more reliable when Signal A shares less of the parameter space with Signal B. If Signal B is allowed to exist at SNRs greater than that of Signal A then the posterior settles on the values of Signal B. The effect of the SNR ratio is shown in Figure 3, where the SNR of Signal B is increased with other signal parameters kept constant.

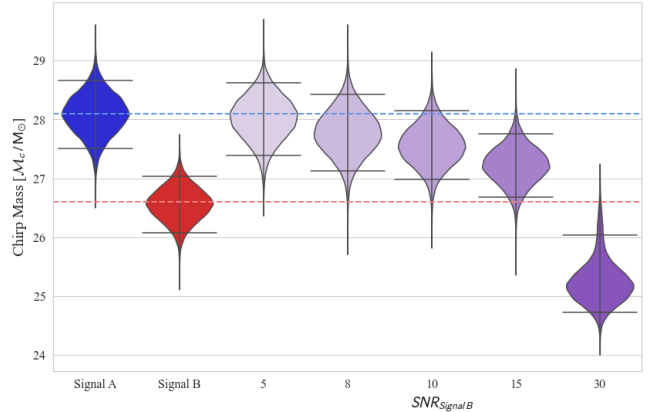


FIG. 3. Recovered chirp mass posterior distributions. Posteriors labeled Signal A and Signal B are for data with a single signal injected at SNR 30. Signal B is injected with a relative merger time of +0.025 seconds and a chirp mass of  $26.6 M_{\odot}$ . The next five posteriors have the two signals injected with the same properties but with the SNR of Signal B varying from 5 to 30. Signal A is kept with SNR of 30 in all runs. The two horizontal lines in blue and red show the injected values of the chirp mass for Signal A and Signal B respectively.

All plots presented here will be posterior distributions of parameters, in the form of violin plots. The first two posteriors will show the posterior distributions for separate, single signal, runs of Signal A and Signal B. The posteriors that follow these are for two overlapping signals of near identical parameters, but with stated differences. Horizontal grey lines show the 90% credible intervals for the posteriors. The two horizontal lines in blue and red show the injected values for the parameter for Signal A and Signal B respectively. All posterior plots were made using the parameter estimation software, *PESummary* [47].

When the two signals have a time separation greater than the period in which the signal is in the detector then the sampler will favour the louder signal. In this situation the signals would have been recorded as separate detections and would not be studied with wide enough time priors to cover both signals.

In the situation where Signal A is both louder than Signal B and merges at a later time, the recovered posterior is much closer to that of Signal A. This is because most of the power is within the period of Signal A. However, if Signal B merges after Signal A, the posterior is more likely to recover significant bias, even at lower SNR ratios. The reverse is true if the relative SNRs of the two signals are swapped.

When signals do overlap in the time domain there

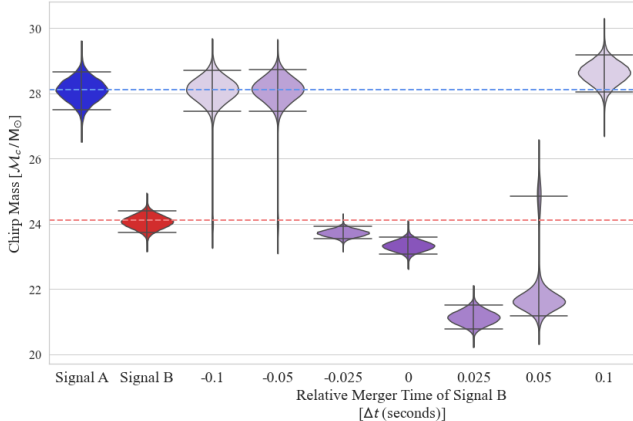


FIG. 4. Recovered chirp mass posteriors. Posteriors labeled Signal A and Signal B are for data with a single signal injected at SNR 30. Signal B is injected with SNR 30 and a chirp mass of  $24.1 M_{\odot}$ . The next seven posteriors have the two signals injected with the same properties but with the relative merger time of the secondary varying. The two horizontal lines in blue and red show the injected values of the chirp mass for Signal A and Signal B respectively.

will always be some bias in the parameter estimation. The bias from time overlap increases as the merger times of the two signals are brought closer together. Figure 4 shows the recovered posteriors for the chirp mass of near identical runs where the SNR of Signal B is constant, but the time separation of the mergers varies between runs.

For highly overlapping signals, the significance of the bias is dominated by the frequency evolution of the signals. This is amplified if the signals are close in the frequency domain. If the parameters of the two systems are such that they have a very different frequency profiles, for instance if they have very different chirp masses, then the sampler struggles to build waveform templates that match the wide variations in frequency. The sampler is therefore more likely to match to the louder signal. On the other hand, if the signals have similar frequency evolution then the power in the signals are combined and the sampler has an easy job matching the signals.

The highly overlapping case, in which the two signals have similar SNRs, frequency profiles and merger times, is shown in Figure 5. Here there are ten, near, identical runs of the same signal configuration. The wild difference between the recovered posteriors is due to the initial phase of Signal B, which was drawn randomly for each run. Figure 5 shows how much effect the phase has in the highly overlapping case.

In the case of high time-SNR-frequency overlap, the

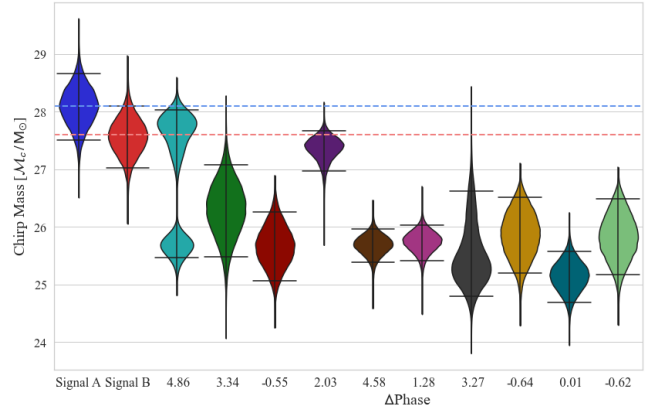


FIG. 5. Recovered chirp mass posteriors. All runs are identical with Signal B of chirp mass  $27.6 M_{\odot}$ , relative merger time of  $-0.025$  seconds and SNR 30. The overlapping signal posteriors differ due to the initial phase of Signal B, which was selected at random from a uniform distribution. The two horizontal lines in blue and red show the injected values of the chirp mass for Signal A and Signal B respectively.

sampler has to fit to a waveform that is varying significantly in frequency space. It therefore, often picks waveforms that are precessing. This leads to samples that have very uneven mass ratios. This is shown in Figures 6 and 7, where the recovered values of mass ratio and  $\chi_p$  are shown as the SNR of Signal B is increased. The apparent precession caused by overlapping signals is a similar process to one described in [48]. In this paper they model precession with the beating of two non-precessing signals. Here we have shown that this can occur from two overlapping signals that are visible in the detector.

## B. LIGO-Virgo Network Runs

Single detector events are rarely published and should always be treated carefully. To examine the more likely case where two overlapping signals are observed in a network of detectors we performed a similar set of injections into three detectors. Two of these detectors were located at the two aLIGO sites in Hanford, Washington and Livingston, Louisiana. These detectors were given an aLIGO design PSD from the penultimate column of the Table given in [46]. The third detector was located in Pisa, Italy and given a PSD of the Advanced Virgo detector at design sensitivity. This PSD was taken from the penultimate column of the Table in [49].

In these runs Signal A's parameters were identical

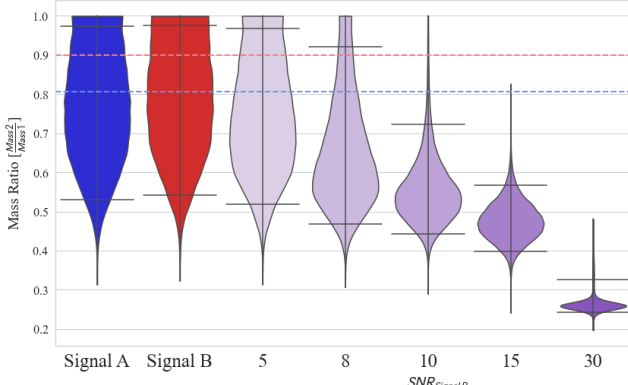


FIG. 6. A plot of posteriors for recovered mass ratio. Here Signal B has chirp mass  $26.6 M_{\odot}$  relative merger time of  $+0.025$  seconds compared to Signal A. The numerically labelled posteriors are at different injected SNRs of Signal B. Signal A has SNR 30 throughout. The two horizontal lines in blue and red show the injected values of the mass ratio for Signal A and Signal B respectively.

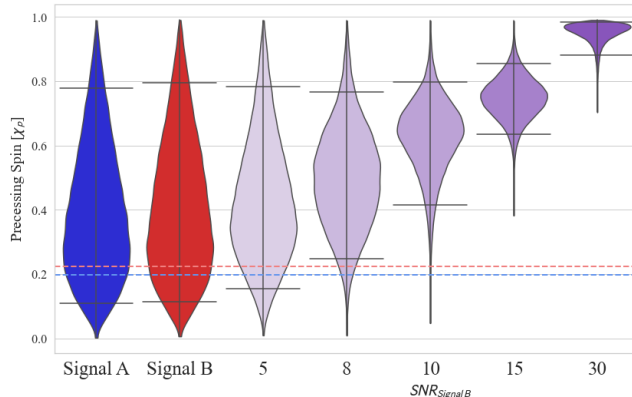


FIG. 7. A plot of posteriors for recovered  $\chi_p$ . Here Signal B has chirp mass  $26.6 M_{\odot}$  relative merger time of  $+0.025$  seconds compared to Signal A. The numerically labelled posteriors are at different injected SNRs of Signal B. Signal A has SNR 30 throughout. The two horizontal lines in blue and red show the injected values of  $\chi_p$  for Signal A and Signal B respectively.

to those in the single detector runs, as outlined in section III. Signal B was allowed to vary in luminosity distance such that it went from one thirtieth to twice the SNR of Signal A. Runs were performed at a variety of different time separations and phases, but with a single Chirp Mass for Signal B of  $24.1 M_{\odot}$ .

In multi-detector networks the position of the true signal in the sky controls the time of arrival at each detector. The difference in arrival time between detectors

is that of the light travel time between the detectors at a given sky location and arrival time. The maximum difference is between the LIGO: Hanford and the Virgo site in Pisa, this is approximately 27.3 ms. This time separation - sky location dependency means that signals that overlap in the detector interfere differently in different detectors and have different merger time separations in each detector.

Due to this sky location dependency we draw up two cases. The best case, in which the two signals arrive at the detectors from two positions at opposite sides of the line connecting LIGO: Hanford and Virgo. This maximises the difference in arrival time between detectors to 54.6 ms, twice the travel time between them. This situation should lead to the smallest bias causing overlap region and are the most likely overlapping events to be recognised and separated.

We also examine the case in which the two signals arrive from the same sky location, but different luminosity distances. These signals arrive at a constant separation independent of detector. These signals should appear more similar to real signals due to the inter-detector consistency. It should be noted that these 'worst case scenario' events are more likely than the best case events. This is because for the merger times to be consistent across the network the signals can either arrive from the same sky location or come from a location perpendicular to the line of sight between detectors. These two scenarios show the extremes of the overlap for detectors based in their current locations.

### 1. Best Case Scenario

We simulate signals at two sky locations at opposite sides of the line of sight between LIGO: Hanford and Virgo. Each signal was created at several time separations,  $\Delta t = [-0.1, 0.1]$ , as set in the Hanford detector. The resulting Virgo time separations are approximately  $\Delta t = [-0.155, 0.045]$ . The time separations in LIGO: Livingston also differ slightly from the Hanford values.

For each of these cases four randomly selected values for the phases were given to Signal B. The chirp mass of Signal B was kept to  $24.1 M_{\odot}$ . The same assumption-less, wide prior set and the same marginalisations were used as in the single detector runs.

In these runs the sampler tends to recover a GW150914-like event for pretty much all the cases in which Signal B merges before the merger of Signal A. In these situations the recovered signal is closer to the parameters of whichever signal is louder in the detector network. This is most likely due to the majority of the

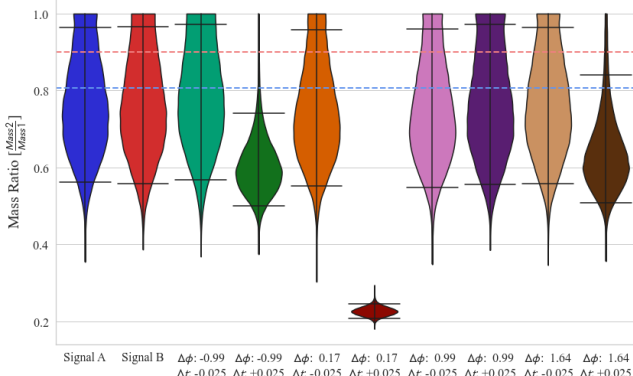


FIG. 8. Recovered Mass ratio posteriors for Signal B overlapping either 0.025 seconds before or after Signal A at a variety of initial phases, injected into a LIGO-Virgo network. Signal B was injected with an SNR of 25. The sky locations of the two systems of Signal A and Signal B were selected to maximise the travel time between the LIGO: Hanford and Virgo detectors. Stated relative merger times apply to the Hanford detector. The two horizontal lines in blue and red show the injected values of the mass ratio for Signal A and Signal B respectively.

power of Signal B being disguised by the more significant Signal A. This is increased by the time separation skewing to before Signal A for the majority of the runs due to the sky location and separation in Virgo.

The recovered posteriors show most evidence of bias in overlapping situations where Signal B merges after Signal A. This can be seen in Figures 8 and 9. These show the recovered mass ratio and luminosity distance posterior distributions for the case where Signal B has an SNR of 25 and merges at time separations of  $\pm 0.025$  seconds, relative to Signal A. It can be seen that, in the case where Signal B merges 0.025 seconds after Signal A, in the LIGO: Hanford detector, the bias is much larger than for the equivalent case of earlier merger. At wider time separations the recovery skews towards a GW150914-like event, although significant bias still occurs in some events.

However, we find that in all of these runs there is still significant bias in runs that merge with a small time separation. As with the single detector analysis, the bias is reduced at wider time separations and at less even SNR ratios. Effects such as recovered precession and well constrained values of mass ratio, as found in single detector runs, are also present in these highly overlapping network events.

As in the single detector runs the recovered signal appears highly precessing. With mass ratio and  $\chi_p$  constrained away from 1 and 0 respectively. To account

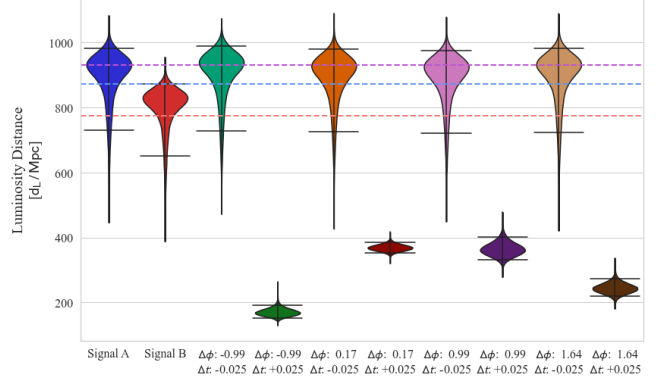


FIG. 9. Recovered luminosity distance posteriors for Signal B overlapping either 0.025 seconds before or after Signal A at a variety of initial phases, injected into a LIGO-Virgo network. Signal B was injected with an SNR of 25. The sky locations of the two systems of Signal A and Signal B were selected to maximise the travel time between the LIGO: Hanford and Virgo detectors. Stated relative merger times apply to the Hanford detector. The two horizontal lines in blue and red show the injected values of the luminosity distance for Signal A and Signal B respectively. The final horizontal line shows the injected luminosity distance for Signal B in the combined runs at the lower SNR.

for this the sampler selects waveforms that look like an edge on system. The sampler therefore predicts that all the power of the signal is in the plus polarisation and leaves little in the cross polarisation. The luminosity distance is therefore recovered to be much smaller than the real value, in order to account for the high SNR.

## 2. Worst Case Scenario

We performed runs in which the two signals merge at the same location in the sky, relative to the detectors. This situation is the most likely to cause a signal that is not recognised as overlapping due to the relative merger time remaining constant regardless of detector. The relative merger times of these signals are constant.

Here we find similar results to those in the section IV B 1, however, we find that the observed bias is much larger and skews away from the recovery of a GW150914-like event, particularly in the situation where Signal B merges after Signal A, relative to the detectors. These results are shown in Figures 10 and 11.

Similar runs were performed with only the two aLIGO detectors at design sensitivity. The posterior distributions of these runs had the same qualitative

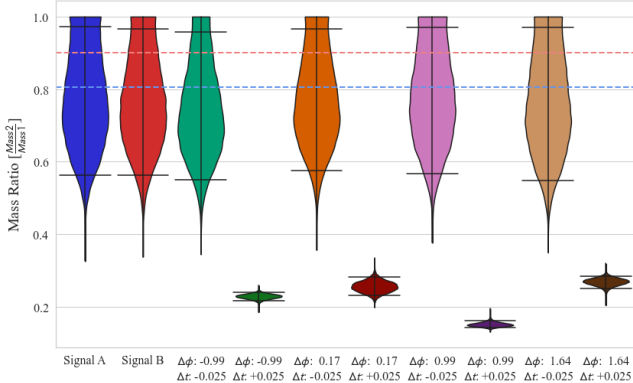


FIG. 10. Recovered Mass ratio posteriors for Signal B overlapping either 0.025 seconds before or after Signal A at a variety of initial phases, injected into a LIGO-Virgo network. Signal B was injected with an SNR of 25. The sky locations of the two events are identical creating identical arrival times at all three detectors. The two horizontal lines in blue and red show the injected values of the mass ratio for Signal A and Signal B respectively.

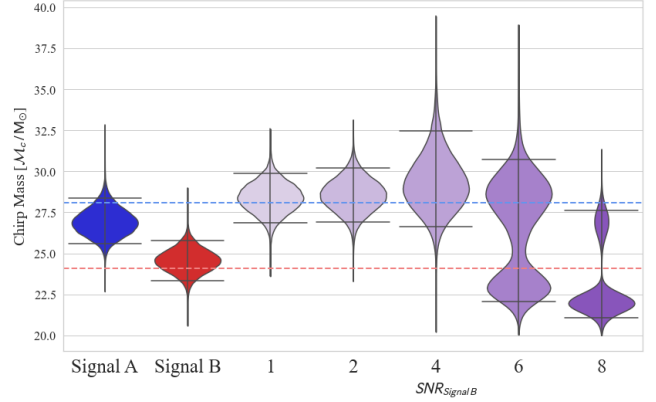


FIG. 12. Recovered chirp mass posteriors for Signal B overlapping either 0.025 seconds after Signal A at a variety of different SNRs, injected into a LIGO-Virgo network. The values given for each posterior are the SNR of Signal B in the LIGO: Hanford detector. Signal A was injected with an SNR of 8. The two horizontal lines in blue and red show the injected values of the chirp mass for Signal A and Signal B respectively.

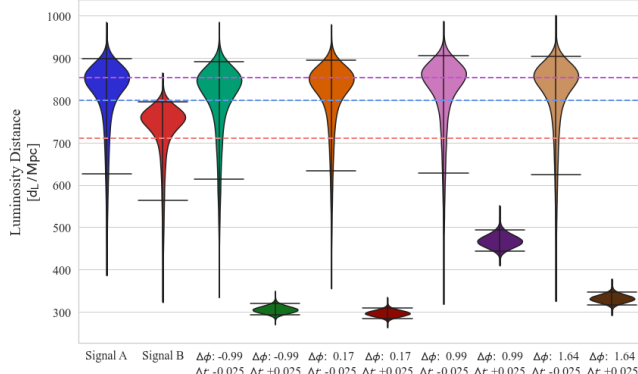


FIG. 11. Recovered luminosity distance posteriors for Signal B overlapping either 0.025 seconds before or after Signal A at a variety of initial phases, injected into a LIGO-Virgo network. Signal B was injected with an SNR of 25. The sky locations of the two events are identical creating identical arrival times at all three detectors. The two horizontal lines in blue and red show the injected values of the luminosity distance for Signal A and Signal B respectively. The final horizontal line, purple, shows the injected luminosity distance for Signal B in the combined runs at the lower SNR.

results but with less precise constraints on certain parameters, as expected with fewer detectors.

### C. Events Below the Detection Threshold

It is possible that signals can be biased by the presence of a second signal, even if that signal were not detectable itself. To test this we performed PE on systems where the Signal A was identical to the GW150914-like signal described previously, but with an SNR of 8 in the LIGO: Hanford detector. This is often regarded as the threshold SNR for signal detection in an individual detector [24].

In this analysis Signal B merged 0.025 seconds after Signal A in order to provide significant bias. Runs were performed with increasing SNR for Signal B from 1 to 8. These runs were performed for the full, three detector LIGO-Virgo network at design sensitivity. The network SNR of Signal A was 13.3, slightly higher than the network SNR threshold of 12 [24]. Sky locations were defined such as to give the two signals a consistent relative merger time across the network of detectors.

The posterior distributions for the chirp mass of these runs are given in Figure 12. These posteriors show that, while these signals are not detectable, they can still cause significant bias in the recovery of Signal A when approaching equal SNR. Such signals would also cause bias in the recovery of a louder Signal A, however, this would not be as significant an issue due to the largely uneven ratio of SNRs.

#### D. LIGO-Voyager Network Runs

Identical runs to the three detector aLIGO network, worst case scenario, were performed with a LIGO-Voyager detector sensitivity. The network kept the same locations as the two aLIGO detectors in Hanford and Livingston, with identical signal parameters. A third detector at LIGO-Voyager sensitivity was not included in the location of the Virgo detector as no current plans for such a detector were available.

Two sets of runs, identical to those described in IV B, were performed. These runs were performed with two differences. The aLIGO design PSD was replaced with a predicted LIGO-Voyager PSD. The PSD used was created from an estimate of the noise budget calculated through the python package `pygwinc` [26].

One set of runs kept the low frequency cut off equal to that of the aLIGO network runs, 20 Hz, the other reduced this to 10 Hz, as expected for LIGO-Voyager. The increase in detector sensitivity, combined with identical parameters to the aLIGO network runs, produces signals with much greater significance in the LIGO-Voyager detector. However, it is the relative SNR that is relevant in these situations. This remains constant.

The results of these runs did not differ greatly from those of the aLIGO network. The recovered posteriors were much more precise than from the aLIGO runs, particularly for the mass ratio, Figure 13. Better constraints of the posteriors were found in the 10 Hz runs than the 20 Hz runs. This is due to the increased number of cycles visible in the detector. This increased number of cycles also shows more interference between overlapping signals. As such the 10 Hz runs show more bias from overlapping signals than the 20 Hz runs in all scenarios.

Example posteriors of the 10 Hz runs are shown in Figures 13 and 14. These show identical runs from the 10 Hz LIGO-Voyager runs as are shown in Figures 10 and 11 for the aLIGO network, worst case scenario.

#### V. PROBABILITY RE-ESTIMATION

Our original investigation into the probability of overlapping signals shows that these events are unlikely to occur until the end of the second generation of GW interferometers. We find that, in a years observations with LIGO-Voyager, there should be  $2^{+2}_{-1}$  overlapping BBH events and around  $46^{+72}_{-27}$  BBH events that merge during the observable period of a BNS merger. However, our study into parameter estimation of such events shows that the signals need to be within approx-

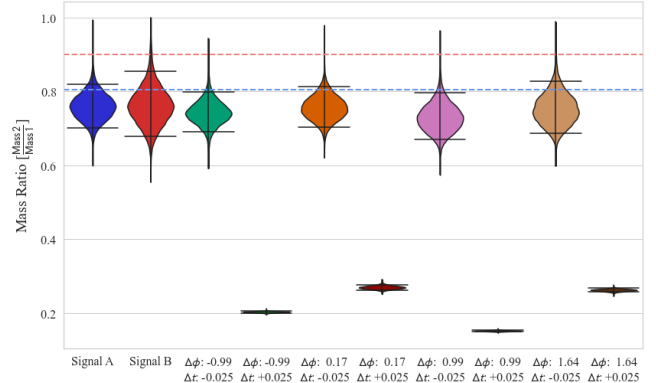


FIG. 13. Recovered Mass ratio posteriors for Signal B overlapping either 0.025 seconds before or after Signal A at a variety of initial phases, injected into a LIGO-Voyager network. These plots are for the equivalent runs in the aLIGO network, given in Figure 10. The two horizontal lines in blue and red show the injected values of the mass ratio for Signal A and Signal B respectively.

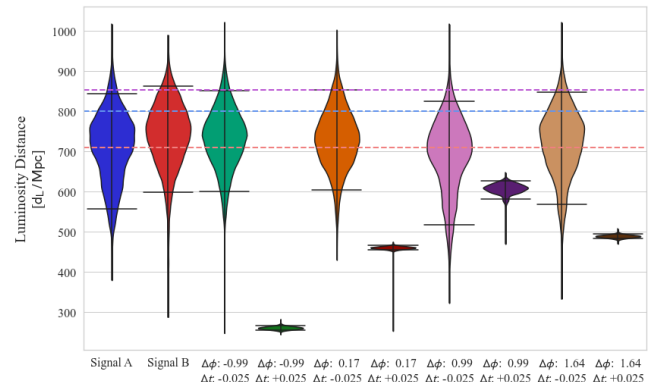


FIG. 14. Recovered luminosity distance posteriors for Signal B overlapping either 0.025 seconds before or after Signal A at a variety of initial phases, injected into a LIGO-Voyager network. These plots are for the equivalent runs in the aLIGO network, given in Figure 11. The two horizontal lines in blue and red show the injected values of the luminosity distance for Signal A and Signal B respectively.

imately  $\pm 0.1$  seconds in merger times in order to cause significant bias. Here we consider what effect this has on the probability of observing overlapping signal bias.

We follow a similar analytical process to that outlined in II A. However, to enforce the bias-time difference constraint we shorten the periods of the signals to 0.2 seconds in length. Applying this constraint we find that approximately  $5400^{+8600}_{-3200}$  BBH mergers will

show significant bias<sup>1</sup> in one year of ET observations. This accounts for approximately  $0.41^{+0.26}_{-0.15}\%$  of BBH mergers. Even half a percent of BBH events showing significant bias could cause significant biases in studies of precessing black hole systems and further population studies.

The value of  $5400^{+8600}_{-3200}$  significant bias, BBH mergers does not account for more than two signals overlapping the signal. We find negligible probability of three or more signals overlapping within  $\sim 0.2$  seconds, even in third generation detectors. However, our statement of significant bias only applies to two signal overlaps. It is likely that multiple signals polluting the signal will cause significant deviations from the true waveform that current parameter estimation techniques will struggle to account for.

## VI. CONCLUSION & FUTURE WORK

Our analysis shows that, although we are unlikely to observe overlapping signals within the lifetime of current detectors, we should expect such events to occur in observations in LIGO-Voyager. This is most likely to occur in the case of BNS+BBH overlaps. However, we do not expect these events to produce significant bias due to the significant differences in their frequency evolution. Unless the merger times are within  $\sim 0.1$  seconds of each other; the sampler will recover a largely unbiased signal. This signal should be one which best fits the given mass prior.

We find that overlapping signals will be present in small numbers by the end of the second generation with LIGO-Voyager. We also find that third generation detectors, such as Einstein Telescope, will be so sensitive that they are unlikely to ever observe signals that do not overlap with multiple other signals. However, due to the requirement of close merger times and high relative SNR, many signals should remain recoverable to a reasonable approximation.

We also predict that LIGO-Voyager should detect several overlapping BBH events. While a few, low overlap, cases may not be a significant problem, their presence could cause trouble for studies of Binary Black Hole populations and tests of General Relativity. In the case of detecting a highly overlapping event; the system could appear highly precessing leading to a further detailed analysis and publication. These events

may affect any further astrophysical studies. We have only considered this for single event cases and leave the effects on population studies for future works.

Overall we find that overlapping BBH mergers do not show significant bias unless their waveforms overlap significantly in time and frequency. The ratio of the SNRs of the two signals must also be fairly even, as high as 0.3, for the sampler to recover signals that differ significantly from the true posterior of the louder signal. Generally bias is more significant if the quieter signal merges after the primary signal.

It is reasonable to assume that most early detections of overlapping BBH mergers will not show significant bias. They should, however, only recover the louder signal. To recover the quieter signal new analysis techniques must be found to sample over the parameter space of two signals.

In a network of detectors the relative sky locations of the two signals, and their relation to the line of sight between the detectors, has an effect upon the significance of the bias. We find that signals in sky locations along the line of sight between two detectors have a smaller region of significant bias. However, if the signals are in locations perpendicular to the line of sight, or at similar sky locations, the bias is more significant.

In the situation of two highly overlapping waveforms the position and distribution of the posterior varies wildly with respect to the initial phase of the two waveforms. In these scenarios the sampler often selects waveforms that match highly precessing signals. This is due to the modulation of the frequencies present in the combined waveform. The result is often systems with mass ratios well constrained and away from the even case. The sampler will then put the majority of the power into the cross polarisation and compensate by constraining a low luminosity distance.

We find that biases from overlapping signals can occur even if the quieter signal causing the bias is itself undetectable. Detections of events with low SNRs should be treated with caution due to the possibility of bias from an undetectable signal.

The results for LIGO-Voyager show that, while higher-sensitivity detectors are more likely to detect bias, they also are more likely to present significant biases in detections. If these can be properly characterized it should be possible to establish which detections contain a potential overlap. It may be necessary to look closely at any events that show significant evidence of precession or uneven mass ratios.

Our analysis of the effects of overlapping waveforms has been confined to the case of overlapping BBH mergers. We don't expect to observe the overlap of BNS systems until significant improvements are made in low-

---

<sup>1</sup> It should be noted that this number also applies to the number of BBH events that overlap BNS mergers, as both signals have an overlap-bias period of  $\sim 0.2$  seconds

frequency detector sensitivity. This limits the observation of such overlaps until third generation detectors.

We did not examine the case of a BBH signal overlapping the merger of a BNS signal. However, we expect that the mergers of BBH events that occur within the inspiral of BNS events should not be recoverable unless they are much louder than the BNS signal. When this is not true, the BNS signal should be fairly easy to recover correctly due to its much longer visible period.

For the less likely case that a BNS merger contains a BBH merger we expect the signals to not be recoverable. It may be possible to correctly recover the BNS from its inspiral. It may further be possible to use the inspiral to predict the merger of the BNS. In this case it can be removed from the data to reveal the BBH merger for further analysis. This could be a viable method of distinguishing such events and we leave this for future analysis.

We do not present any complete methods for proving that a detected signal is biased by another. Neither

do we present methods of sampling these situations to distinguish between the signals. However, we have expect that it may be possible to do so by comparing the appearance of the waveform between the two detectors and examining the cases of highly precessing, highly polarised signals.

## VII. ACKNOWLEDGEMENTS

We would like to thank Charlie Hoy and Duncan Macleod for invaluable programming assistance. We would also like to thank Fabio Antonini and Geraint Pratten for useful discussions. We are grateful for computational resources provided by Cardiff University, and funded by an STFC grant supporting UK Involvement in the Operation of Advanced LIGO. This work was supported in part by STFC grant ST/V001396/1. The work has been allocated the internal LIGO Document number LIGO-P2100074.

---

[1] Junaid Aasi, BP Abbott, Richard Abbott, Thomas Abbott, MR Abernathy, Kendall Ackley, Carl Adams, Thomas Adams, Paolo Addesso, RX Adhikari, et al. Advanced ligo. *Classical and quantum gravity*, 32(7):074001, 2015.

[2] Fet al Acernese, M Agathos, K Agatsuma, D Aisa, N Allemandou, A Allocca, J Amarni, P Astone, G Balestri, G Ballardin, et al. Advanced virgo: a second-generation interferometric gravitational wave detector. *Classical and Quantum Gravity*, 32(2):024001, 2014.

[3] Benjamin P Abbott, R Abbott, TD Abbott, MR Abernathy, F Acernese, K Ackley, C Adams, T Adams, P Addesso, RX Adhikari, et al. Binary black hole mergers in the first advanced ligo observing run. *Physical Review X*, 6(4):041015, 2016.

[4] Benjamin P Abbott, R Abbott, TD Abbott, MR Abernathy, F Acernese, K Ackley, C Adams, T Adams, P Addesso, RX Adhikari, et al. Gw150914: The advanced ligo detectors in the era of first discoveries. *Physical review letters*, 116(13):131103, 2016.

[5] Benjamin P Abbott, Rich Abbott, TD Abbott, Fausto Acernese, Kendall Ackley, Carl Adams, Thomas Adams, Paolo Addesso, RX Adhikari, VB Adya, et al. Gw170817: observation of gravitational waves from a binary neutron star inspiral. *Physical Review Letters*, 119(16):161101, 2017.

[6] BP Abbott, Richard Abbott, TD Abbott, S Abraham, F Acernese, K Ackley, C Adams, RX Adhikari, VB Adya, C Affeldt, et al. Gwtc-1: a gravitational-wave transient catalog of compact binary mergers ob- served by ligo and virgo during the first and second observing runs. *Physical Review X*, 9(3):031040, 2019.

[7] Fausto Acernese, M Agathos, L Aiello, A Allocca, A Amato, S Ansoldi, S Antier, M Arène, N Arnaud, S Ascenzi, et al. Increasing the astrophysical reach of the advanced virgo detector via the application of squeezed vacuum states of light. *Physical review letters*, 123(23):231108, 2019.

[8] M Tse, Haocun Yu, Nutsinee Kijbunchoo, A Fernandez-Galiana, P Dupej, L Barsotti, CD Blair, DD Brown, SE Dwyer, A Effler, et al. Quantum-enhanced advanced ligo detectors in the era of gravitational-wave astronomy. *Physical review letters*, 123(23):231107, 2019.

[9] Aaron Buijema, Craig Cahillane, GL Mansell, CD Blair, R Abbott, C Adams, RX Adhikari, A Ananyeva, S Appert, K Arai, et al. Sensitivity and performance of the advanced ligo detectors in the third observing run. *Physical Review D*, 102(6):062003, 2020.

[10] R Abbott, TD Abbott, S Abraham, F Acernese, K Ackley, A Adams, C Adams, RX Adhikari, VB Adya, C Affeldt, et al. Gwtc-2: Compact binary coalescences observed by ligo and virgo during the first half of the third observing run. *arXiv preprint arXiv:2010.14527*, 2020.

[11] Alexander H Nitz, Thomas Dent, Gareth S Davies, Sumit Kumar, Collin D Capano, Ian Harry, Simone Mozzon, Laura Nuttall, Andrew Lundgren, and Márton Tápai. 2-ogc: Open gravitational-wave catalog of binary mergers from analysis of public advanced ligo

and virgo data. *The Astrophysical Journal*, 891(2):123, 2020.

[12] Tejaswi Venumadhav, Barak Zackay, Javier Roulet, Liang Dai, and Matias Zaldarriaga. New binary black hole mergers in the second observing run of advanced ligo and advanced virgo. *Physical Review D*, 101(8):083030, 2020.

[13] Barak Zackay, Tejaswi Venumadhav, Liang Dai, Javier Roulet, and Matias Zaldarriaga. Highly spinning and aligned binary black hole merger in the advanced ligo first observing run. *Physical Review D*, 100(2):023007, 2019.

[14] Barak Zackay, Liang Dai, Tejaswi Venumadhav, Javier Roulet, and Matias Zaldarriaga. Detecting gravitational waves with disparate detector responses: two new binary black hole mergers. *arXiv preprint arXiv:1910.09528*, 2019.

[15] Vishal Baibhav, Emanuele Berti, Davide Gerosa, Michela Mapelli, Nicola Giacobbo, Yann Bouffanais, and Ugo N Di Carlo. Gravitational-wave detection rates for compact binaries formed in isolation: Ligo/virgo o3 and beyond. *Physical Review D*, 100(6):064060, 2019.

[16] Raymond Robie, Aidan Brooks, Christopher Wipf, Koji Arai, and Rana Adhikari. Ligo voyager: A cryogenic silicon interferometer for gravitational-wave detection. *Bulletin of the American Physical Society*, 65, 2020.

[17] Stefan Hild, Simon Chelkowski, Andreas Freise, Janyce Franc, Nazario Morgado, Raffaele Flaminio, and Riccardo DeSalvo. A xylophone configuration for a third-generation gravitational wave detector. *Classical and Quantum Gravity*, 27(1):015003, 2009.

[18] M Punturo, M Abernathy, F Acernese, B Allen, Nils Andersson, K Arun, F Barone, B Barr, M Barsuglia, M Beker, et al. The einstein telescope: a third-generation gravitational wave observatory. *Classical and Quantum Gravity*, 27(19):194002, 2010.

[19] David Reitze, Rana X Adhikari, Stefan Ballmer, Barry Barish, Lisa Barsotti, GariLynn Billingsley, Duncan A Brown, Yanbei Chen, Dennis Coyne, Robert Eisenstein, et al. Cosmic explorer: the us contribution to gravitational-wave astronomy beyond ligo. *arXiv preprint arXiv:1907.04833*, 2019.

[20] Elia Pizzati, Surabhi Sachdev, Anuradha Gupta, and Bangalore Sathyaprakash. Bayesian inference of overlapping gravitational wave signals, 2021.

[21] Anuradha Samajdar, Justin Janquart, Chris Van Den Broeck, and Tim Dietrich. Biases in parameter estimation from overlapping gravitational-wave signals in the third generation detector era, 2021.

[22] LIGO Scientific Collaboration. Instrument science white paper. *LIGO Document: LIGO*, 1400316, 2015.

[23] R Abbott, TD Abbott, S Abraham, F Acernese, K Ackley, A Adams, C Adams, RX Adhikari, VB Adya, C Affeldt, et al. Population properties of compact objects from the second ligo-virgo gravitational-wave transient catalog. *arXiv preprint arXiv:2010.14533*, 2020.

[24] Benjamin P Abbott, R Abbott, TD Abbott, S Abraham, F Acernese, K Ackley, C Adams, VB Adya, C Affeldt, M Agathos, et al. Prospects for observing and localizing gravitational-wave transients with advanced ligo, advanced virgo and kagra. *Living reviews in relativity*, 23(1):1–69, 2020.

[25] LIGO-P2000434-v1: Data Release for "Population properties of compact objects from the second LIGO-Virgo Gravitational-Wave Transient Catalog", 2021.

[26] LIGO Scientific Collaboration. pygwinc: <https://git.ligo.org/gwinc/pygwinc>, 2021.

[27] Hsin-Yu Chen, Daniel E Holz, John Miller, Matthew Evans, Salvatore Vitale, and Jolien Creighton. Distance measures in gravitational-wave astrophysics and cosmology. *Classical and Quantum Gravity*, 38(5):055010, 2021.

[28] Jolien Creighton Jameson Rollins. Inspiral-range: <https://git.ligo.org/gwinc/inspiral-range>, 2021.

[29] R Abbott, TD Abbott, S Abraham, F Acernese, K Ackley, C Adams, RX Adhikari, VB Adya, C Affeldt, M Agathos, et al. Gw190412: Observation of a binary-black-hole coalescence with asymmetric masses. *Physical Review D*, 102(4):043015, 2020.

[30] Bhaskar Biswas, Rana Nandi, Prasanta Char, Sukanta Bose, and Nikolaos Stergioulas. Gw190814: On the properties of the secondary component of the binary. *arXiv preprint arXiv:2010.02090*, 2020.

[31] Ingo Tews, Peter TH Pang, Tim Dietrich, Michael W Coughlin, Sarah Antier, Mattia Bulla, Jack Heinzel, and Lina Issa. On the nature of gw190814 and its impact on the understanding of supranuclear matter. *The Astrophysical Journal Letters*, 908(1):L1, 2021.

[32] Pau Amaro-Seoane, Heather Audley, Stanislav Babak, John Baker, Enrico Barausse, Peter Bender, Emanuele Berti, Pierre Binetruy, Michael Born, Daniele Bortoluzzi, et al. Laser interferometer space antenna. *arXiv preprint arXiv:1702.00786*, 2017.

[33] Mark Hannam, Patricia Schmidt, Alejandro Bohé, Leila Haegel, Sascha Husa, Frank Ohme, Geraint Pratten, and Michael Pürrer. Simple model of complete precessing black-hole-binary gravitational waveforms. *Physical review letters*, 113(15):151101, 2014.

[34] Bohé, Alejandro and Hannam, Mark and Husa, Sascha and Ohme, Frank and Pürrer, Michael and Schmidt, Patricia. Phenomv2 - technical notes for lal implementation. Technical Report LIGO-T1500602, LIGO Project, 2016.

[35] Sascha Husa, Sebastian Khan, Mark Hannam, Michael Pürrer, Frank Ohme, Xisco Jiménez Forteza, and Alejandro Bohé. Frequency-domain gravitational waves from nonprecessing black-hole binaries. i. new numerical waveforms and anatomy of the signal. *Physical Review D*, 93(4):044006, 2016.

[36] Sebastian Khan, Sascha Husa, Mark Hannam, Frank Ohme, Michael Pürrer, Xisco Jiménez Forteza, and Alejandro Bohé. Frequency-domain gravitational

waves from nonprecessing black-hole binaries. ii. a phenomenological model for the advanced detector era. *Physical Review D*, 93(4):044007, 2016.

[37] Geraint Pratten, Cecilio García-Quirós, Marta Colleoni, Antoni Ramos-Buades, Héctor Estellés, Maite Mateu-Lucena, Rafel Jaume, Maria Haney, David Keitel, Jonathan E Thompson, et al. Let's twist again: computationally efficient models for the dominant and sub-dominant harmonic modes of precessing binary black holes. *arXiv preprint arXiv:2004.06503*, 2020.

[38] Cecilio García-Quirós, Marta Colleoni, Sascha Husa, Héctor Estellés, Geraint Pratten, Antoni Ramos-Buades, Maite Mateu-Lucena, and Rafel Jaume. Multimode frequency-domain model for the gravitational wave signal from nonprecessing black-hole binaries. *Physical Review D*, 102(6):064002, 2020.

[39] Sebastian Khan, Frank Ohme, Katerina Chatzioannou, and Mark Hannam. Including higher order multipoles in gravitational-wave models for precessing binary black holes. *Physical Review D*, 101(2):024056, 2020.

[40] Serguei Ossokine, Alessandra Buonanno, Sylvain Marsat, Roberto Cotesta, Stanislav Babak, Tim Dietrich, Roland Haas, Ian Hinder, Harald P Pfeiffer, Michael Pürrer, et al. Multipolar effective-one-body waveforms for precessing binary black holes: Construction and validation. *Physical Review D*, 102(4):044055, 2020.

[41] Patricia Schmidt, Frank Ohme, and Mark Hannam. Towards models of gravitational waveforms from generic binaries: II. modelling precession effects with a single effective precession parameter. *Physical Review D*, 91(2):024043, 2015.

[42] Jolien DE Creighton and Warren G Anderson. *Gravitational-wave physics and astronomy: An introduction to theory, experiment and data analysis*. John Wiley & Sons, 2012.

[43] Duncan M Macleod, Joseph S Areeda, Scott B Coughlin, Thomas J Massinger, and Alexander L Urban. Gwpy: a python package for gravitational-wave astrophysics. *SoftwareX*, 13:100657, 2021.

[44] Gregory Ashton, Moritz Hübner, Paul D Lasky, Colm Talbot, Kendall Ackley, Sylvia Biscoveanu, Qi Chu, Atul Divakarla, Paul J Easter, Boris Goncharov, et al. Bilby: A user-friendly bayesian inference library for gravitational-wave astronomy. *The Astrophysical Journal Supplement Series*, 241(2):27, 2019.

[45] Joshua S Speagle. dynesty: a dynamic nested sampling package for estimating bayesian posteriors and evidences. *Monthly Notices of the Royal Astronomical Society*, 493(3):3132–3158, 2020.

[46] LIGO Scientific collaboration. aLIGO Design PSD: [https://dcc.ligo.org/public/0094/P1200087/042/fig1\\_aligo\\_sensitivity.txt](https://dcc.ligo.org/public/0094/P1200087/042/fig1_aligo_sensitivity.txt), 2017.

[47] Charlie Hoy and Vivien Raymond. Pesummary: the code agnostic parameter estimation summary page builder. *arXiv preprint arXiv:2006.06639*, 2020.

[48] Stephen Fairhurst, Rhys Green, Charlie Hoy, Mark Hannam, and Alistair Muir. Two-harmonic approximation for gravitational waveforms from precessing binaries. *Physical Review D*, 102(2):024055, 2020.

[49] LIGO Scientific collaboration. adVirgo Design PSD: [https://dcc.ligo.org/public/0094/P1200087/042/fig1\\_adv\\_sensitivity.txt](https://dcc.ligo.org/public/0094/P1200087/042/fig1_adv_sensitivity.txt), 2017.